Optimum Control of Cavity Flow

Rasika Fernando[2], Denis Sipp[1], Anton Lebedev[1] & Laurent Jacquin[1]

[1] *: Office National d'Etudes et de Recherches Aérospatiales*
Département d'Aérodynamique Fondamentale et Expérimentale
8, Rue des Vertugadins 92190 MEUDON
sipp@onera.fr

[2] *: Institut Jean le Rond d'Alembert*
UMR CNRS 7190
Université Pierre et Marie Curie
4, Place Jussieu 75252 PARIS
fernando@lmm.jussieu.fr

Abstract :

For high Reynolds numbers $Re = U_\infty L/\nu$, with an order of magnitude of a few thousands, a flow over a square cavity becomes unsteady with the growth of two-dimensional instabilities. This phenomenon is studied by computing : 1/ the branch of steady solutions with respects to the Reynolds number, using a branch tracking method ; 2/ the eigenvalues and eigenvectors of the global linearized operator with respects to Re. We thus show that the cavity is subject to a Hopf bifurcation at a critical Reynolds number denoted by Re_c. After setting the computations in a supercritical case for which $Re > Re_c$, we use an optimum control algorithm to minimize the energy of the perturbations at various terminal times T. The control will consist in unsteady blowing and succion on the cavity wall. We will analyze the phenomenology of the control law with a description of the influence of the target time T and the cost of the control which will be denoted by m.

Résumé :

Lorsque le nombre de Reynolds $Re = UL/\nu$ est suffisamment élevé, de l'ordre de quelques milliers, l'écoulement affleurant une cavité de rapport d'aspect $L/D = 1$ devient instationnaire bidimensionnel. Ce phénomène est étudié en recherchant : 1/ la branche de solutions stationnaires en fonction du nombre de Reynolds à l'aide d'une méthode de suivi de branche ; 2/ les valeurs et modes propres de l'opérateur linéarisé global en fonction de Re. On montre ainsi que la cavité subit une bifurcation de Hopf à un certain nombre de Reynolds critique Re_c. Puis, en se plaçant dans un cas supercritique $Re > Re_c$, on met en œuvre le formalisme du contrôle optimal pour minimiser l'énergie des perturbations instables à un temps horizon T variable. Le moyen de contrôle choisi est constitué de soufflages / aspirations instationnaires le long de la paroi de la cavité. On finira par une analyse physique de la loi de contrôle obtenue en décrivant l'importance du paramètre m du coût du contrôle.

Key-words :

cavity flow ; global instability ; optimum control

1 Introduction

The interaction of a fluid with a mechanical structure can be fatal, under certain flow regimes, to the integrity of the latter. In order to keep a structure from buffeting, it is thus essential to control the interacting flow.

In the case of a driven cavity flow, the buffeting was first explained by Rossiter (1964) as the effect of a feedback loop where self-sustained oscillations are due to the emission of acoustic waves from the leading edge of the cavity. A better understanding of the phenomena had been brought later on by Bilanin *et al*. (1973), when a greater importance was given to the role

played by the mixing layer in the excitation of the leading edge. It has been shown by Tam *et al*. (1978) that Rossiter's model predicted the correct tones only in the range of Mach numbers going from 0.4 to 1.2.

The computation of the base flows' eigenvalues and eigenvectors, at various Reynolds numbers, have brought up the existence of a globally unstable mode, above a critical Reynolds number Re_c. This global instability has its origin in the shear layer (or Kelvin-Helmholtz) instability and its growth is responsible for the unsteadyness of the flow.

The aim of this article is to present the adjoint based optimum control algorithm (as described by Bewley (2001)) used to minimize the energy of the perturbations of a supercritical mode ($Re = 7500$) at a terminal time T for a cost m. This is done by applying an unsteady blowing and suction control law at the cavity wall.

2 Presentation of the geometry and computation of the base flows

We consider an open square cavity in a uniform stream of velocity U_∞. In the following, all quantities are made non-dimensional with these two reference length and velocity scales. The two-dimensional homogeneous incompressible Navier-Stokes equations then read :

$$\partial_t \mathbf{u} + \nabla \mathbf{u} \cdot \mathbf{u} + \nabla p - Re^{-1} \nabla^2 \mathbf{u} = 0 \ \text{ and } \ \nabla \cdot \mathbf{u} = 0 \tag{1}$$

where $\mathbf{u} = (u, v)$ denote longitudinal and transverse velocity components and p the pressure of the flow field. Re is the Reynolds number based on the length scale L and the velocity U_∞.

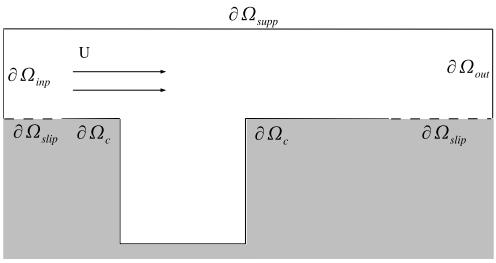

Figure 1: Geometry of the computational domain Ω. $\partial\Omega_{inp}$, $\partial\Omega_{out}$ and $\partial\Omega_{supp}$ are the input, output and upper boundaries. The cavity surface is presented by the solid boundaries $\partial\Omega_{slip}$ and $\partial\Omega_c$, where the former is a slipping boundary and the latter a non-slipping boundary. The use of a slipping boundary is to move away the origin of the boundary layer from the input and output boundaries so that it has the least possible interaction with these. A longitudinal unitary velocity is applied on the input boundary $\partial\Omega_{inp}$ ($u = 1; v = 0$) and a symetry condition ($v = 0$) is applied on the upper boundary $\partial\Omega_{supp}$. The condition on the output boundary $\partial\Omega_{out}$ is relaxed.

Figure 1 presents the computational domain in which the following steady base flow equations (2) are solved using a mixed finite element method (P1 elements for the pressure field and P2 elements for the velocity components) :

$$(\mathbf{U} \cdot \nabla)\, \mathbf{U} + \nabla P - Re^{-1} \nabla^2 \mathbf{U} = 0 \ \text{ and } \ \nabla \cdot \mathbf{U} = 0, \tag{2}$$

which gives

$$F(\mathbf{Q}) = 0, \tag{3}$$

where $\mathbf{Q} = (\mathbf{U}, P) = (U, V, P)$.

Equation (3) is solved using Newton's method in order to have an accurate solution for the base flow. To initiate the computation, a converged direct simulation solution at a low Re is

required as the initial "guess value ". The branch of the Reynolds numbers is then followed and base flow solutions for various Re are obtained as shown on Figure 2.

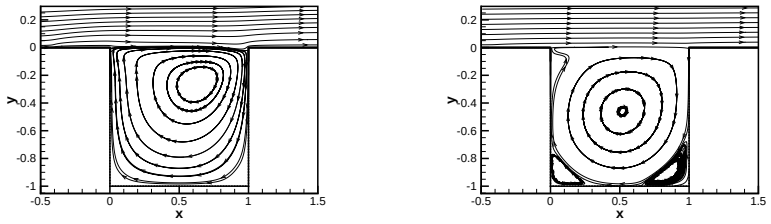

Figure 2: Streamtraces for $Re = 250$ (left) and $Re = 7500$ (right). We observe on these figures that the cavity flow is composed of two regions : an outer flow and a recirculation bubble inside de cavity. For $Re = 250$ we can see that the bubble is driven by the outer flow because of the high viscosity, whereas for $Re = 7500$ the axis of the bubble is centered inside the cavity. Furthermore, for high Re, three minor recirculation bubbles appear in the lower and upper left corners of the cavity. It is the beating of this mixing layer which will produce the vortices, which are convected downstream by the outer flow and which, by hitting the cavity leading edge produce the feedback effect.

The use of the Newton's method is essential in this case studied here since the unsteady nature of the flow makes it impossible to obtain converged solutions by a direct numerical simulation.

3 Global stability analysis

To investigate the two-dimensional linear global stability of the base flow to disturbances, we decompose the velocity and pressure fields $\mathbf{q} = (\mathbf{u}, p) = (u, v, p)$ into a steady base flow $\mathbf{Q}$, to which is superimposed a perturbation $\varepsilon\mathbf{q}' = \varepsilon(\mathbf{u}', p') = \varepsilon(u', v', p')$ of amplitude $\varepsilon \ll 1$. We thus obtain the linearized Navier-Stokes equations : $\mathbf{A}\cdot\mathbf{q}' = \partial_t\mathbf{B}\cdot\mathbf{q}'$, which solutions at leading order ε are sought in the form of normal modes : $\mathbf{q}'(x, y, t) = \hat{\mathbf{q}}(x, y)\exp(\sigma_r t)\exp(i\sigma_i t)$, with the trivector $\hat{\mathbf{q}} = (\hat{\mathbf{u}}, \hat{p}) = (\hat{u}, \hat{v}, \hat{p})$, the eigenvector or global mode, associated to the complex eigenvalue $\sigma = \sigma_r + i\sigma_i$, the global growth rate. By replacing in the linearized Navier-Stokes equations, we obtain the system $\mathbf{A}\cdot\hat{\mathbf{q}} = \sigma\mathbf{B}\cdot\hat{\mathbf{q}}$, which is solved using the shift-invert Arnoldi's method. We thus compute the solutions (σ_r, σ_i) and Figure 3 presents one of the unstable mode corresponding to $\sigma_r = 0.89$ and $\sigma_i = 10.9$.

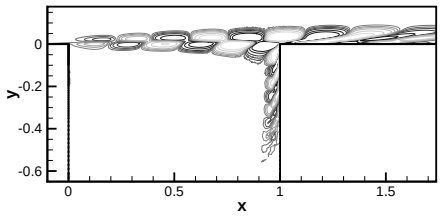

Figure 3: Vorticity of the unstable mode at $Re = 7500$. We can see here unstable structures correspondingto Kelvin-Helholtz type instabilites.

4 Optimum Control

4.1 Fundamentals

The computation of the optimum control law is achieved by minimizing the cost functional :

$$J(f,g) = \int\int_{\Omega} [u(f,g,T)^2 + v(f,g,T)^2]\, dx\, dy + \frac{m^2}{T} \int_0^T\int_{\partial\Omega_c} [f(s,t)^2 + g(s,t)^2] ds\, dt, \quad (4)$$

where the first term accounts for the energy of the perturbations at the terminal time T and the second for the cost of the control. We denote by $\mathbf{c}(s,t) = (f(s,t), g(s,t))$ the longitudinal and transverse velocities of the blowing and suction at the cavity wall and s is the coordinate along the cavity wall. The cost of the control m is a cost per unit of time and is given arbitrarily. The higher m the more expensive is the control.

J is then minimized using its gradient ∇J, which gives the direction of the descent, and an optimal step α, which is the "distance" to go along this direction.

The computation of ∇J requires the computation of the adjoint state variables, which are computed backward in time from $t = T$ to $t = 0$. After setting an arbitrary initial control law ($\mathbf{c}^0 = 0$ for instance), we then compute at each iteration a new control law $\mathbf{c}^{n+1} = \mathbf{c}^n + \alpha^n \nabla J^n$.

4.2 Analysis of the control mechanism

The following computations were made with a terminal time $T = 4$ and cost $m = 141$.

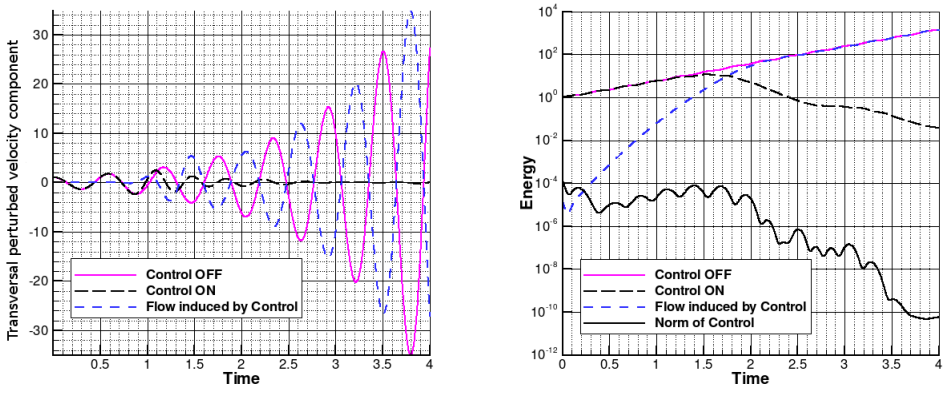

Figure 4: Evolution of the transversal component of the perturbed velocity v in the center of the shear layer (left figure) and of the energy of the perturbations (right figure) in a time interval from $t_i = 0$ to $t_f = T = 4$. The solid pink line corresponds to the case without control, the dashed black line to the controlled configuration. The dashed blue line is the flow induced by the wall control. The solid black line on the right figure is a plot of the norm of the control on the cavity wall.

The initial condition for the computation of the linearized equations is the unstable mode whose vorticity is shown in Figure 3. We can clearly observe on Figure 4 that the perturbations grow freely when no control is applied on the cavity wall.

To understand the control mechanism, a homogeneous problem is also solved (zero initial condition) where only the unsteady optimum control is applied on the cavity wall. The transverse velocity of the flow induced by the control grows with its phase being opposite to that of the solution of the linearized problem. The sum of these two solutions shows the effect

of the optimal control on the evolution of an unstable mode and we can clearly see that the perturbations are destroyed when the optimum control law is applied on the cavity wall.

The unstable nature of this mode is also shown by the energy plot (Figure 4 on the right). The energy of the flow field induced by the control in the homogeneous computation is low in the first half of the simulation because of the zero initial condition, but as expected, it catches up on the energy of the freely evolving perturbations, which confirms the fact that the induced field reconstructs the opposite of the solution of the linearized Navier-Stokes equations.

The energy of the optimally controlled perturbation field, shown by the dashed black line of the right figure, decreases drastically instead of growing like that of the freely evolving perturbations.

4.3 Parametric study

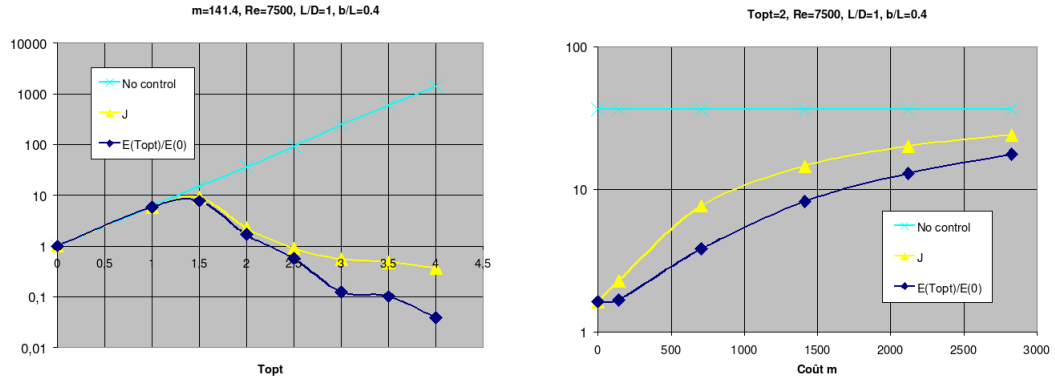

Figure 5: Energy at terminal time $t = T$ (normalized by the energy at $t = 0$) for various values of T at a fixed $m = 141.4$ (left figure), and energy at terminal time $T = 2$ for various values of the cost m (right figure). The blue-green line is a plot of the energy a T when no control is applied and the perturbed field is left to evolve freely, the dark blue line is the normalized energy of the controlled flow at $t = T$ and the yellow line represents the values of the cost functional J.

The graph on the left gives the final energy of the perturbations in the controlled and uncontrolled cases as a function of the terminal time T. It shows that for a fixed cost, the control starts to be efficient for terminal times greater than 1.5. Then, the greater the terminal time, the greater the reduction of the energy.

For terminal times smaller than 1.5, we can see that the energy of the controlled perturbations at $t = T$ is the same as that of the freely evolving perturbations. This is due to the fact that the control on the upstream wall has not enough time to reach the downstream corner of the cavity, where the eigen mode is strongest. Hence, the cavity flow displays a delay time of about $T = 1.5$ for control to be efficient. This time is approximately equal to the convection time of a vortical structure along the cavity, since its velocity is about $1/2$.

On the other hand for a terminal time fixed at $T = 2$, we can see that the control becomes more and more effective as $m \to 0$. Also, for an expensive control, we observe that the reduction of the cost functional becomes small.

5 Conclusions

In this work we have first computed the base flows for various Reynolds numbers ranging from $Re = 250$ to $Re = 7500$ and we have shown the existance of globally unstable modes for

supercritical Reynolds numbers, whose free evolution in time leads to an exponential increase of the energy of the perturbations. This phenomenon is responsible for the unsteadying of the flow and the buffeting of the structure, and needs thus to be controlled.

The control medium used is blowing and succion at the cavity wall governed by an unsteady optimum control law and computed by an iterative method in which a cost functional is minimized. This control law is such that it reconstructs the opposite of the pertubation flow field. The resulting perturbation field is thus almost zeroed.

In order to have the most efficient control, we need to adjust the cost m and terminal time T parameters accordingly. We have shown that the control was the most efficient for long terminal times ($T > 1.5$) and for values of m small enough to let the control act sufficently on the perturbation field.

References

Bewley, T.R 2001 Flow Control : new challenges for a new Renaissance. *Prog. Aero. Sci.* **37** 21-58

Bilanin, A.J., Covert E.E. 1973 Estimation of possible excitation frequencies for shallow rectangular cavities *AIAA Journal* **11** 347-351

Rossiter, J.E 1964 Wind tunnel experiments of the flow over rectangular cavities at subsonic and transonic speeds. *Aeronautical Reserch Council.* Report and Memorandum n˚3438

Tam, C., Block, P. 1978 On the tones and pressure oscillations induced by flow over rectangular cavities *J. Fluid Mech.* **89** 373-399